An Investigation of Shock-Cylinder Interaction

J.G. Oakley, B.P. Puranik, M.H. Anderson,
R.R. Peterson, R. Bonazza,
R.P. Weaver, M.L. Gittings

July 1999

UWFDM-1116

Prepared for the 22nd International Symposium on Shock Waves, Imperial College, London, UK, July 18-23, 1999.

FUSION TECHNOLOGY INSTITUTE

UNIVERSITY OF WISCONSIN

MADISON WISCONSIN

An Investigation of Shock-Cylinder Interaction

J.G. Oakley[1], B.P. Puranik[1], M.H. Anderson[1], R.R. Peterson[1], R. Bonazza[1], R.P. Weaver[2], M.L. Gittings[2]

1. Department of Engineering Physics, University of Wisconsin-Madison, Madison, WI 53706, USA
2. Los Alamos National Laboratory, Los Alamos, NM 87545, USA

Abstract: An experimental and numerical investigation of the interaction of a shock wave with a hollow cylinder is undertaken, to model the impulsive loading of the cooling tubes for proposed inertial confinement fusion (ICF) reactors. These tubes constitute the first structural wall of these reactors. As the shock traverses the cylinder, pressure-time histories are recorded at seven azimuthal locations with flush mounted piezoelectric pressure transducers on the surface of the cylinder. Two accelerometers are placed inside the hollow of the cylinder to measure the lateral and vertical acceleration of the cylinder. Imaging of the flow and shock diffraction patterns is performed with shadowgraphy. Experimental measurements are compared with numerical simulations performed using an Eulerian code, RAGE.

Key words: Shock Wave Reflections, Impulsive Loading, Shock Diffraction

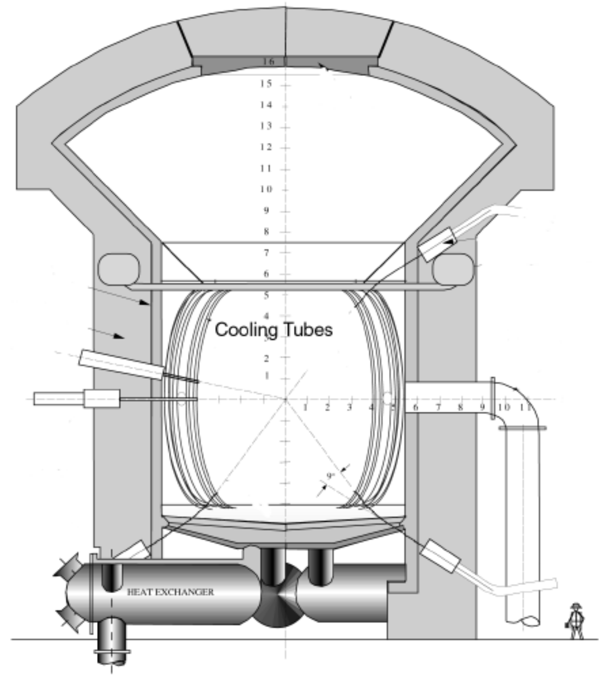

Figure 1. Schematic of the LIBRA-SP Target Chamber Design

1. Introduction

The use of light ion, heavy ion, electron beam or laser driven inertial confinement fusion (ICF) has received renewed interest with the development of the National Ignition Facility (NIF). In addition to the many neutronic and magnetohydrodynamic hurdles inherent in ignition, there are hydrodynamic issues that need to be resolved for the cooling of ICF reactors (LIBRA, LIBRA-LiTE, LIBRA-SP, BLASCON, HYLIFE-I, HIBALL, and others) (Kulcinski et al. (1994), Moir (1996)). These hydrodynamic issues are well suited for studying in a shock tube.

1.1. Impulsive Shock Loading on Cooling Tubes

Recent studies concerning the protection of the first structural wall of the ICF reactors have been conducted leading to the proposal of INPORT (INhibited Flow in POROus Tube) and rigid PERIT (PErforated RIgid Tube) units (Kulcinski et al. (1994)). Figure 1 shows the schematic of the target chamber for the LIBRA-SP reactor and the cooling tubes. The PERIT units are hollow tubes which carry a PbLi eutectic alloy. The INPORT tubes are constructed out of a porous orthogonal weave of SiC, C, or steel which allows an ablative film of the PbLi to form on the outer surface of the tube which absorbs X-rays and target debris while the bulk of the liquid flowing through the tube absorbs the photon and neutron energy and mitigates the isochoric heating by the neutrons. The first few levels of the PERIT cooling arrangement have fan sprays, creating a liquid sheet of PbLi which performs essentially the same task as the film on the INPORT tube design. These tubes must be able to withstand the impact of the shock wave formed by the thermonuclear reaction of the deuterium-tritium (DT) fuel.

Impulsive loading on a cooling tube is studied in a shock tube using a hollow cylinder as a model. The acceleration and vibration of the tubes can be determined by measuring the pressure-time distribution around the cylinder. Bryson and Gross (1961) and Syshchicova et al. (1967) performed studies recording the shock formations at different times after an initial shock-cylinder interaction.

Bishop and Rowe (1967) measured the pressure distribution on a cylinder in a blast channel with piezoelectric pressure transducers; however, due to the limitations of the blast channel, only experiments with low Mach numbers were conducted. Several studies using holographic interferometry (Heilig (1969), Takayama and Itoh (1985)) studied the shock diffraction over a cylinder and estimated the pressure distribution around the cylinder using an equation of state. In an effort to increase the extent of the experimental data base, pressure distributions for strong shocks are measured directly in a large, square inner cross-section shock tube able to achieve Mach numbers on the order of 5 into atmospheric air. The time history of the pressure distribution is recorded with piezoelectric pressure transducers mounted flush on the surface of the cylinder.

2. Experimental Description

The experiments are conducted in the newly fabricated Wisconsin Shock Tube. The tube is vertical, with a large square inner cross-section (25 cm × 25 cm) and is 9.2 m long. The square cross-section provides the parallel walls necessary for flow visualization. The tube has a structural capability to withstand a 20 MPa pressure load. Figure 2 shows the schematic of the shock tube. A detailed description of the shock tube is provided in Oakley et al. (1999).

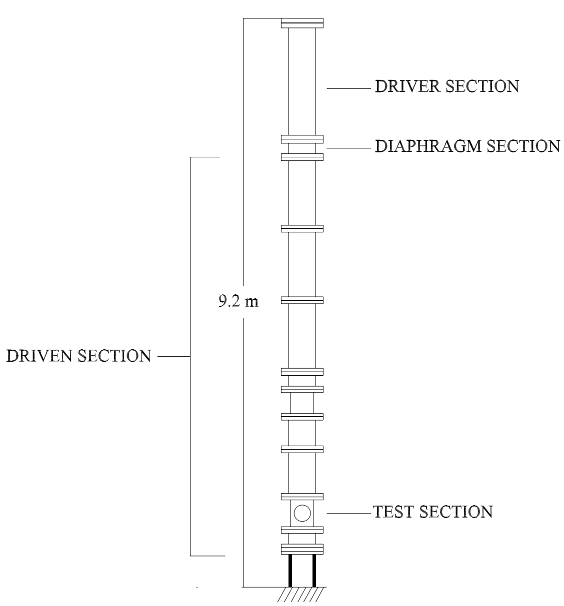

Figure 2. Schematic of the Wisconsin Shock Tube

The shock-loading of an ICF cooling tube is modeled with a 25 cm long, 6.35 cm diameter cylinder, placed in the center of the test section of the shock tube. The 25 cm length completely spans the 25 cm cross-section of the tube and permits a two dimensional fluid dynamics study of the shock-induced transient flow. Two 2.5 cm diameter fixed rods are in place at each end of the cylinder for vertical support during the experiment. The hollow portion of the tube also serves as a cable-way for the transducers' cables. The cables are connected to feed-throughs mounted in the wall of the shock tube. Figure 3 shows the schematic of the cylinder and the support structure arrangement.

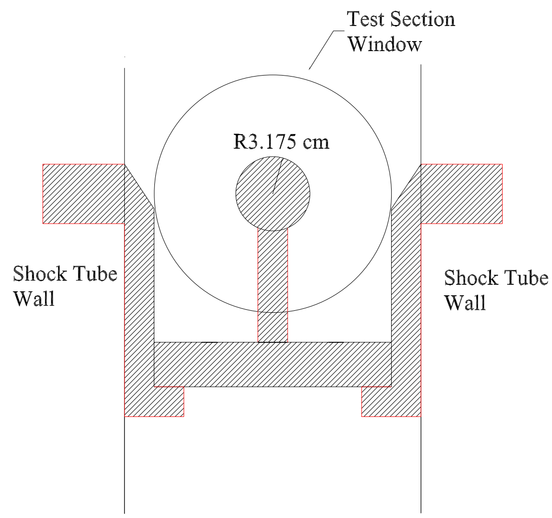

Figure 3. Schematic of the Cylinder and the Support Structure

Shadowgraphy is used for flow visualization. A modified Continuum (Surelite II-PIV) pulsed Nd:YAG laser with a pulse width of 10 ns is used as light source for the imaging. The laser has been modified from its original repetition mode to a "single shot" mode. This allows the laser to stay fully charged and pulse when an external trigger (such as a spike from a piezoelectric pressure transducer signal) is provided during the experimental run. A 16-bit CCD camera (Spectra Video Series, by Pixel Vision) is used to capture the flow field images. It has a back-lit, 1024 × 1024 pixel array, a thermo-electrically cooled sensor and a low speed (40 kHz) transfer rate that minimize low dark current and readout noise (1 e^-/pix s and 5-8 e^- rms respectively, @ -45° C). The incident shock wave, produced as a result of rupture of a steel diaphragm, triggers the laser to pulse and the image is captured by the CCD camera. One image is obtained per experiment. An HP-Infinium 4 channel digital oscilloscope with a sampling rate of 1 GHz per channel is used to record the pressure traces from the piezoelectric pressure transducers.

The laser beam is spatially filtered before it is expanded by a plano-concave lens (focal length -15 mm). It is then collimated by a plano-convex lens (focal length 500 mm) into a parallel beam of diameter 212 mm. The collimated beam is passed through the test section windows and projected on a screen. The camera is focused on the screen and captures the image.

Typically, two piezoelectric transducers are flush mounted in the wall of the shock tube to measure the shock speed and trigger the laser to pulse. In addition, four more are mounted on the cylinder at 0, 30, 60 and 90 degrees, as measured from the topmost point on the cylinder as shown in Fig. 4A. The cylinder can be rotated by 90 degrees and pressures at three more locations can be measured (Fig. 4B), thus giving a total of seven locations around the cylinder (0, 30, 60, 90, 120, 150 and 180 degrees measured from the topmost point on the cylinder). The repeatability in the Mach number for different experiments is ±0.4% and the consistency in the pressure measurement at angular position of 90° for the two orientations of the cylinder has been verified. Two accelerometers are mounted on the cylinder, one in the direction of shock propagation and the other perpendicular to it, to measure the accelerations of the cylinder due to the shock loading.

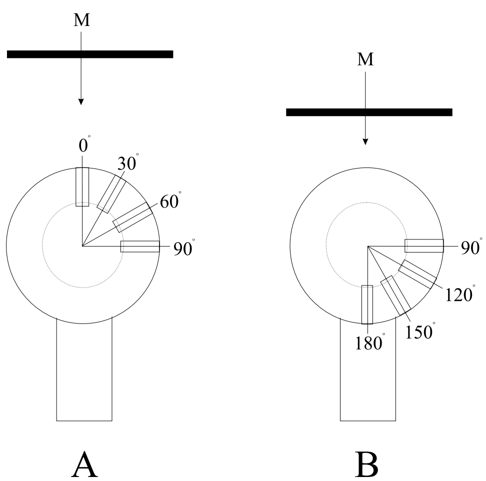

Figure 4. Schematic of the Pressure Transducer Locations on the Surface of Cylinder

3. Numerical Simulation

Numerical hydrodynamic simulations are undertaken to complement the experimental investigations. With the experimental setup only one image is captured per experiment. A simulation, on the other hand, can reveal the flow characteristics for many different times – typically 10-15 for animations. The simulation also provides many other physical characteristics of the flow that are unobtainable with experiment (e.g. temperature, density, vorticity, etc.). For the single cylinder investigations discussed here, the experimental shadowgraphy images are compared to density contour plots generated from the simulation and the cylinder surface pressure data is compared with the pressure data generated from the simulation.

The RAGE (Radiation Adaptive Grid Eulerian) code is employed for the simulations. The code has been used successfullemplooR tained from RAGE simulation of the shock-cylinder interaction. The time delay between the first and second plot is 0.05 ms while that between the first and third plot is 0.09 ms. The simulation image shows that the important characteristics of the reflected and transmitted shocks are captured. The shock reflected off the surface of the cylinder has the same geometry as the experimental image. The location and geometry of the triple point is also captured accurately. The end of the slip line, in contact with the surface of the cylinder, is moving slowly as compared to that in the shadowgraphy images (Fig. 5B).

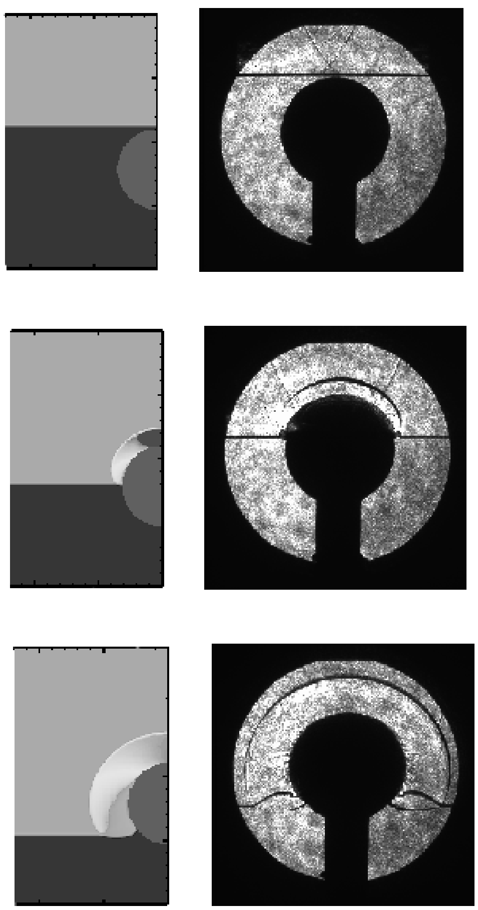

A B

Figure 5. A: Density Contour Plots from the Numerical Simulation Using RAGE at t=0, t=0.03 and t=0.08 ms. B: Successive Shadowgraphs Showing Direct Mach Reflection at t=0, t=0.05 ms and t=0.09 ms

The pressure-time history recorded by the seven transducers, as the shock diffracts over the cylinder, is shown in Fig. 6. Qualitatively, the figure reveals that the maximum pressure occurs at the top of the cooling tube model (normal to the shock) and then decreases as the angle (relative to the upwards vertical) increases. For impulsive force measurements needed for cooling tube design, it is necessary to integrate the pressure history data for each angular segment of the cylinder as a function of time. The maximum pressure occurs "instantaneously" at the top of the tube; however, the force on the tube must be determined by integrating the seven pressure time series over the surface of the tube.

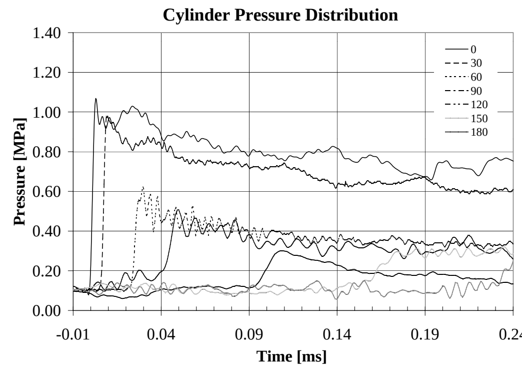

Figure 6. Pressure-Time History for the Surface of the Cylinder for a Mach 1.85 Shock Wave

Figure 7 shows the RAGE simulation results for the pressure-time histories at the same locations as the pressure transducers. In addition, pressure histories at 40° and 50° locations have also been plotted. It can be seen that there is an excellent agreement between the experimental results (Fig. 6) and the RAGE simulations in the prediction of the pressures and the progression of the shock wave along the cylinder.

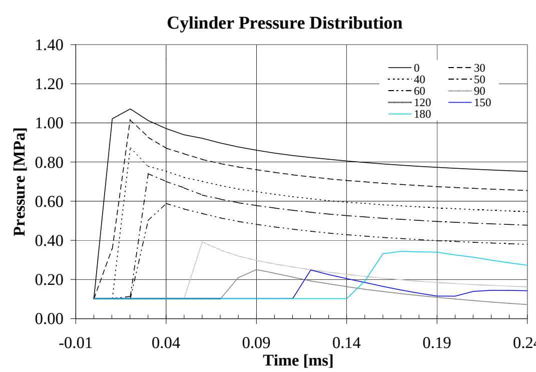

Figure 7. Pressure-Time History from RAGE Simulation for the Surface of the Cylinder for a Mach 1.85 Shock Wave

A critical design parameter for the reactor's cooling tubes is the impulsive loading. The tubes must have sufficient structural integrity to withstand the impulsive loading of the shock wave resulting from the detonation of a deuterium-tritium (DT) fuel pellet. In the series of tests presented here, the impulsive loading is quite high; on the order of that experienced by a golf ball that travels 100 m after being struck with a club. From the pressure data of Fig. 6, it is possible to calculate the impulse by integrating the pressure as a function of angle and time, over the time for which the shock is interacting with the cylinder. It is given by:

$$I = \int_0^{\tau} 2 \int_0^{\theta_m(t)} P(\theta, t) R cos^2(\theta) L d\theta dt \qquad (1)$$

where $P(\theta, t)cos(\theta)$ is the vertical pressure as a function of position and time, $RLcos(\theta)d\theta$ is the area element of the cylinder surface subjected to the pressure, $\theta_m(t)$ is the angle subtended by the shock wave at any given time measured from the vertical central plane, τ is the time for which the shock wave is in contact with the cylinder and the factor of 2 accounts for the symmetrical loading of the cylinder about a vertical central plane. R and L are the radius and the length of the cylinder, respectively.

A pressure history at every 5° interval along the surface of the cylinder is determined by performing a linear interpolation between the closest measured angular pressures for each time interval (i.e. between 0° and 30°, 30° and 60° and so on). The pressure data is integrated from the top of the cylinder to the angle $\theta_m(t)$ to obtain the force. The force applied to the cylinder is integrated from the time the shock first makes contact until it leaves the cylinder to obtain the impulse. A force is still present on the cylinder after the shock has left contact with the cylinder, due to unequal pressures on the top and bottom halves; however, the time of contact between the cylinder and the shock wave serves as an appropriate time to calculate the impulse. The impulse is found to be 0.8271 Ns, giving an average force of 8439.28 N for the 0.098 ms it takes the shock to travel from the top to the bottom of the cylinder. As a quantitative comparison, the impulse calculated from the RAGE simulation yields a value of 0.8703 Ns and an average force of 8880.71 N for the same interaction time. Therefore, the results are within 5.2% of each other. The error may be further reduced by refining the timestep in the RAGE output prior to impulse calculations. Currently the timestep for sampling the output of the RAGE data is 0.01 ms. Figure 8 shows the force as a function of time for both the experimental data and RAGE simulation. As can be seen, there is a good agreement between the experimental and numerical results. A future goal is to develop a relation between the impulsive load, the incident Mach number, and the type of gas the shock is traveling through.

Figure 9 shows the acceleration of the cylinder in the vertical and horizontal directions. The maximum vertical acceleration on the tube is 13,800 g's. This result cannot be used directly because of differences between the cooling tube prototype and the cooling tube model – both in the size of the tube and the manner in which it is supported. However, numerical studies of the structural response of the tube model to impulsive loading are in progress and the results will be compared against the experimental data shown in Fig. 9. Upon such benchmarking, the numerical model will represent a useful design tool for the final cooling tube prototype.

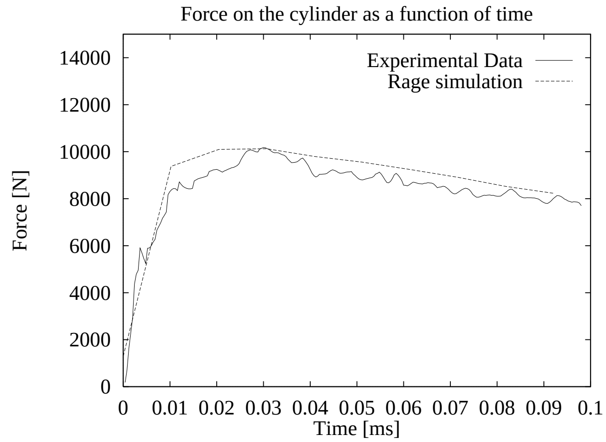

Figure 8. Force Exerted on the Cylinder by the Interaction of the Shock Wave as a Function of Time

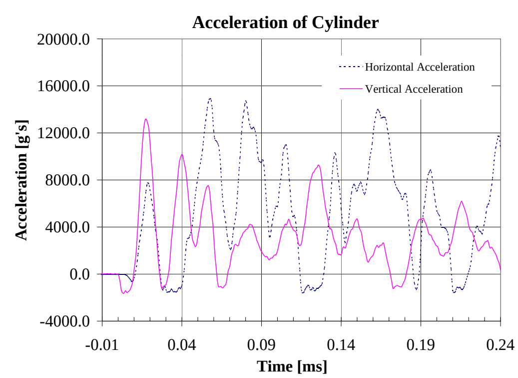

Figure 9. Acceleration-Time History of the Cylinder for a Mach 1.85 Shock Wave

The combination of the dynamic pressure history, acceleration data and optical diagnostics provide a unique experimental characterization of the ICF cooling tube model when subjected to shock loading.

5. Future Work

The primary objective of the preliminary experiments reported in this paper is to validate the hydrodynamics of the numerical code, RAGE, on a simple system such as a single cylinder. In order to model the impulsive loading of the cooling tubes of an ICF reactor more rigorously, future experiments are planned to study the interaction of a shock wave with a bank of hollow cylinders. In particular, an arrangement of three cylinders, as shown in Fig. 10 is being designed presently. This arrangement models the first two structural walls of an ICF reactor. The diameters and the relative distances between the cylinders are such that the geometrical aspects of the cooling tube arrangement in an actual reactor design are reproduced. The cylinders will be placed in the shock tube test section such that the two smaller cylinders are at the top facing the incident shock wave. Shadowgraphy will be used to image the shock diffraction patterns in this complicated interaction. Experimental results will be compared to the results obtained from numerical simulations performed with RAGE.

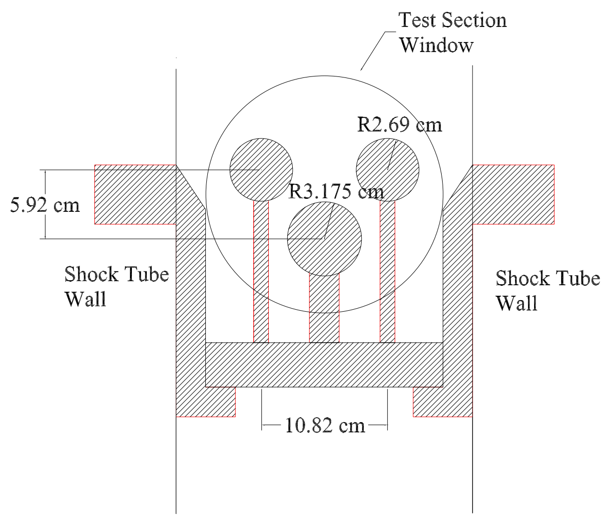

Figure 10. Schematic of the Three Cylinder Arrangement

6. Summary

An experimental and numerical investigation for modeling the impulsive loading of the cooling tubes of future ICF reactors is undertaken. In this first series of experiments, the interaction of a Mach 1.85 shock wave with a single hollow cylinder is studied and the experimental results are compared with numerical simulations using the AMR code, RAGE. In particular, these include the geometric aspects of the diffraction of the shock wave over the cylinder and a comparison of the pressures at seven different azimuthal locations on the surface of the cylinder. The shock diffraction pattern is reproduced accurately with RAGE suggesting a good agreement between the experimental and numerical density fields. There is good agreement for the pressure distribution around the cylinder, and the impulse calculated from the RAGE pressure data is within 5.2% of the value calculated from the experimental data. This indicates an overall good agreement with experimental results. Future experiments and simulations are in progress to study the interaction of a shock wave with a bank of cylinders.

Acknowledgement. The authors would like to thank Paul Brooks for machining and fabrication help. This work was supported by DOE Grant No. DE-FG02-97ER54413.

References

Bishop VJ, Rowe RD (1967) The interaction of a long duration friedlander shaped blast wave with an infinitely long right circular cylinder. Atomic Weapons Research Establishment, Aldermaston, Berkshire, England. AWRE Report No. 0-38/67

Bryson AE, Gross RF (1961) Diffraction of strong shocks by cones, cylinders, and spheres. Journal of Fluid Mechanics, Vol. 10, Part 1:1-23

Goldman SR, Caldwell SE, Wilke MD et al. (1999) Shock structuring due to fabrication joints in targets. Submitted to Physics of Plasmas.

Heilig WH (1969) Diffraction of a shock wave by a cylinder. Physics of Fluids 12, Supplement 1:154-157

Kulcinski GL, Peterson RR, Moses GA et al. (1994) Evolution of light ion driven fusion power plants leading to the LIBRA-SP design. Fusion Technology, Vol.26:849-856

Moir RW (1996) Liquid wall inertial fusion energy power plants. Fusion Engineering and Design 32-33:93-104

Oakley JG, Puranik BP, Anderson MH, Peterson RR, Bonazza R (1999) Planar imaging of density interfaces accelerated by strong shocks. ISSW22 paper No. 0170.

Syshchicova MP, Beryozkina MK, Semenov AN. The flow formation around a body in a shock tube (in Russian). Collection of papers: the aerophysical investigation of supersonic flows, Science publishers, Moscow:7-13

Takayama K, Itoh K (1985) Unsteady drag over cylinders and aerofoils in transonic shock tube flows. Proceedings of the 15th ISSW:479-485

Weaver RP, Gittings ML, Baltrusaitis RM, Zhang Q, Sohn S (1997) 2D and 3D simulations of RM instability growth with RAGE: a continuous adaptive mesh refinement code. Proceedings of the 21st ISSW, Paper No. 8271

Weaver RP, Gittings ML, Clover MR (1999) The parallel implementation of RAGE: a 3D continuous adaptive mesh refinement shock code. ISSW22 paper No. 3560